

No snow-plough mechanism during the rapid hardening of supermassive black hole binaries

Clément Baruteau^{1*}, Enrico Ramirez-Ruiz² and Frédéric Masset³

¹*DAMTP, University of Cambridge, Wilberforce Road, Cambridge CB3 0WA, UK*

²*Department of Astronomy and Astrophysics, University of California, Santa Cruz, CA 95064, USA*

³*Instituto de Ciencias Físicas, UNAM, Apdo. Postal 48-3, 62251-Cuernavaca, Morelos, México*

Accepted 2012 March 19. Received 2012 February 21; in original form 2012 January 03

ABSTRACT

We present two-dimensional hydrodynamical simulations of the tidal interaction between a supermassive black hole binary with moderate mass ratio, and the fossil gas disc where it is embedded. Our study extends previous one-dimensional height-integrated disc models, which predicted that the density of the gas disc between the primary and the secondary black holes should rise significantly during the ultimate stages of the binary’s hardening driven by the gravitational radiation torque. This snow-plough mechanism, as we call it, would lead to an increase in the bolometric luminosity of the system prior to the binary merger, which could be detected in conjunction with the gravitational wave signal. We argue here that the snow-plough mechanism is unlikely to occur. In two-dimensions, when the binary’s hardening timescale driven by gravitational radiation becomes shorter than the disc’s viscous drift timescale, fluid elements in the inner disc get funneled to the outer disc through horseshoe trajectories with respect to the secondary. Mass leakage across the secondary’s gap is thus found to be effective and, as a result, the predicted accretion disc luminosity will remain at roughly the same level prior to merger.

Key words: accretion, accretion discs — black hole physics — gravitational waves — hydrodynamics — methods: numerical

1 INTRODUCTION

The merger of two galaxies results in the formation of a newly assembled galaxy containing a supermassive black hole binary in its nucleus (Begelman et al. 1980). Models of hierarchical galaxy formation predict that the most common supermassive black hole binaries arise from minor galactic mergers, and have unequal-mass black holes (Lacey & Cole 1993). The tidal interaction between the binary black hole, and the disc of gas and stars it is embedded in, shrinks the binary’s orbit. The hardening efficiency has a complex dependence on the binary’s mass ratio (Kazantzidis et al. 2005), the gas disc-to-binary mass ratio (Lodato et al. 2009), and stellar dynamical interactions (Milosavljević & Merritt 2001). Provided the binary hardens to sufficiently small separations, the angular momentum extracted from the binary’s orbit becomes progressively more dominated by gravitational radiation. When the gravitational wave torque prevails over the disc torque, the disc’s accretion rate becomes much smaller than the binary’s hardening rate.

One-dimensional disc models (Armitage & Natarajan 2002; Lodato et al. 2009; Chang et al. 2010) showed that the

density of the disc region located between the primary and the secondary black holes should significantly increase prior to coalescence, as the binary’s hardening is dominated by gravitational radiation. In this scenario, the secondary rapidly drains the inner disc onto the primary, acting like a snow-plough. The increase in the inner disc density would lead to a sudden increase in the disc’s bolometric luminosity in the few days prior to merger. This would constitute an electromagnetic precursor to a supermassive black hole merger, which could be identified in conjunction with the gravitational wave signal detectable with the Laser Interferometer Space Antenna (LISA) (Chang et al. 2010).

In this Letter, we show that this prediction does not hold in two-dimensional (2D) disc models. We demonstrate with the help of 2D hydrodynamical simulations that when the binary’s hardening is dominated by gravitational radiation, the inner disc is progressively funneled to the outer disc through horseshoe trajectories with respect to the secondary, with the consequence that there should be no significant increase in the disc luminosity prior to the merger. The physical problem we consider is described in § 2, and the numerical setup of our simulations is detailed in § 3. Our results of calculations are presented in § 4, followed by some concluding remarks in § 5.

* E-mail: C.Baruteau@damtp.cam.ac.uk

2 PHYSICAL PROBLEM

We examine the tidal interaction between a supermassive black hole binary with mass ratio $q \ll 1$ and the gaseous disc it is embedded in, neglecting for simplicity the presence of other stars. The torque responsible for the binary's hardening comprises the tidal torque Γ_{disc} exerted by the gaseous disc, and the torque Γ_{GW} due to the emission of gravitational waves (GW). The latter reads (e.g., Armitage & Natarajan 2005)

$$\Gamma_{\text{GW}} = -\frac{32}{5} \frac{G^3}{c^5 a^3} \left[\frac{G(M_1 + M_2)}{a} \right]^{1/2} M_1(M_1 + M_2)M_2^2 \quad (1)$$

for a circular binary, where M_1 and $M_2 = qM_1$ denote the mass of the primary and of the secondary, respectively, a is the binary's semi-major axis, c is the speed of light, and G is the gravitational constant. Since $|\Gamma_{\text{GW}}|$ strongly increases with decreasing a , the binary's hardening is ultimately driven by the gravitational wave torque. The binary's hardening timescale τ_{GW} due to the GW torque is

$$\tau_{\text{GW}} = \frac{5}{256} \frac{c^5 a^4}{G^3} M_1^{-1} M_2^{-1} (M_1 + M_2)^{-1}. \quad (2)$$

Further denoting the Schwarzschild radius $r_g = 2GM_1/c^2$, Eq. (2) can be recast as

$$\frac{\tau_{\text{GW}}}{T_{\text{orb}}} \approx \frac{1.76 \times 10^{-2}}{q\sqrt{1+q}} \left(\frac{a}{r_g} \right)^{5/2}, \quad (3)$$

where T_{orb} is the orbital period at the binary's semi-major axis a . At the innermost stable circular orbit (ISCO), located at $r_{\text{isco}} = 3r_g$ for a non-rotating primary black hole, $\tau_{\text{GW}}/T_{\text{orb}} \approx 2.4, 25$ and 250 for $q = 10^{-1}, 10^{-2}$ and 10^{-3} , respectively.

In this study, the secondary to primary mass ratio is fixed to $q = 2 \times 10^{-2}$, and this large value implies that the secondary is able to open a gap around its orbit even in a relatively thick and viscous disc (Lin & Papaloizou 1986; Crida et al. 2006). It also makes the two-dimensional approximation for the disc applicable when discarding gas accretion onto the secondary (D'Angelo et al. 2005). We point out, as did Gould & Rix (2000), that apart from the presence of the GW torque, the physical problem we consider shares a number of analogies with the orbital evolution of a massive gap-opening planet in a protoplanetary disc.

We examine the evolution of the fluid elements in the inner disc close to the location of the inner separatrix of the secondary's horseshoe region. These fluid elements are on approximately circulating streamlines with respect to the secondary, with a relative (synodic) period $\tau_{\text{syn}} \sim$ half the horseshoe libration period. The horseshoe libration period reads $\tau_{\text{lib}} = 8\pi a \times (3\Omega x_s)^{-1}$, where Ω is the secondary's angular frequency, and x_s is the radial half-width of the horseshoe region. For gap-opening secondaries, $x_s \sim 2R_H$ (Masset et al. 2006), where $R_H = a(q/3)^{1/3}$ is the Hill radius of the secondary.

During a synodic period, if the radial distance δa_b by which the binary hardens becomes comparable to, or greater than the radial distance δa_s by which fluid elements near the inner separatrix drift inward, these fluid elements embark on horseshoe trajectories and are funneled to the outer disc. The value of δa_s is essentially set by the viscous torque, and δa_b by $\Gamma_{\text{disc}} + \Gamma_{\text{GW}} \approx \Gamma_{\text{GW}}$ when the binary shrinkage is dominated by gravitational radiation. Thus, in order of magnitude, $\delta a_b \gtrsim \delta a_s$ when τ_{GW} becomes shorter than the viscous drift timescale $\sim 2a^2/3\nu$, where $\nu = \alpha h^2 a^2 \Omega_K$ is the disc's turbulent viscosity

(α denotes the alpha viscous parameter, h the disc's aspect ratio, and Ω_K the Keplerian angular velocity). Using Eq. (3), the typical binary separation below which $\delta a_b \gtrsim \delta a_s$, often called decoupling radius, can thus be estimated as

$$\frac{a}{r_g} \sim 13 \times \left(\frac{\alpha}{0.03} \right)^{-2/5} \left(\frac{q}{0.02} \right)^{2/5} \left(\frac{h}{0.08} \right)^{-4/5}, \quad (4)$$

where α and h are to be evaluated at the secondary's location. Detailed modeling of the disc's thermal balance yields a decoupling radius that is a few times larger than that given in Eq. (4) (Milosavljević & Phinney 2005). This illustrates that when the hardening of an unequal-mass binary black hole is dominated by gravitational radiation, a substantial funneling of the inner disc to the outer disc is possible beyond the ISCO location, which we confirm with 2D hydrodynamical simulations in § 4.

3 PHYSICAL MODEL AND NUMERICAL SETUP

We investigate the tidal interaction between a black hole binary and the gas disc it is embedded in, assuming the binary's hardening is dominated by the emission of gravitational waves. For this purpose, 2D hydrodynamical simulations were carried out with the FARGO code (Masset 2000, <http://fargo.in2p3.fr>). A cylindrical coordinate system $\{r, \varphi\}$ centred onto the primary black hole is adopted. The disc extends from $r = 1.2r_g$ to $r = 35.4r_g$ (that is, $r \in [0.4 - 11.8]r_{\text{isco}}$ with assuming a non-rotating primary).

Binary parameters— The mass of the primary and secondary black holes is $M_1 = 5 \times 10^8 M_\odot$ and $M_2 = qM_1 = 10^7 M_\odot$, respectively, as in Armitage & Natarajan (2002). The initial semi-major axis of the binary is $a_0 \approx 11.8r_g \approx 5.7 \times 10^{-4}$ pc (or, $a_0 \sim 4r_{\text{isco}}$). The binary is assumed to be circular, and its orbital plane to be aligned with the disc. Each black hole is treated as a point mass potential. Relativistic effects are discarded for simplicity and to facilitate comparison with previous studies. Similarly, gas accretion onto the secondary is neglected. Also, to avoid a large accumulation of mass inside its Hill radius, the secondary's gravitational potential is smoothed over a softening length $\varepsilon = H(a_0)$, where H is the pressure scale height (its value is specified below).

Disc parameters— The disc is initially axisymmetric and rotates at the angular frequency $\Omega(r)$ about the primary. The expression for $\Omega(r)$ assumes a radial equilibrium between the centrifugal acceleration, the radial acceleration due to the pressure gradient, and the gravitational acceleration due to the primary alone. The initial gas density is $\approx 10^7 \text{ g cm}^{-2} \times (r/a_0)^{-1/2}$, which corresponds to an initial mass $\approx 6.5 \times 10^{-4} M_1$. For simplicity, a locally isothermal equation of state is considered where the initial radial profile of the disc temperature, which we take proportional to $r^{-3/2}$, remains stationary. The disc temperature is conveniently related to the disc's aspect ratio $h = H/r$, which we take to be $h(r) = 0.08 \times (r/a_0)^{-1/4}$. The disc turbulence is modeled with a constant kinematic viscosity ν that corresponds to an alpha parameter $\alpha \approx 0.03$ uniformly throughout the disc.

Numerical setup— The grid has $N_r = 280$ cells along the

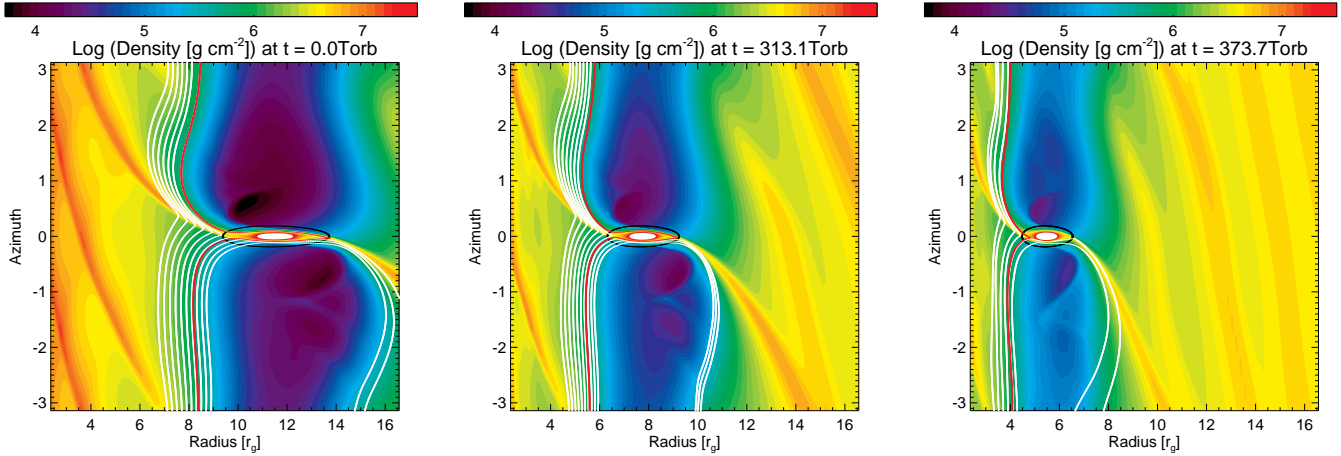


Figure 2. Time sequence of the gas surface density when the binary’s hardening is driven by the GW torque. The x -axis shows the radial coordinate in units of the Schwarzschild radius r_g (part of the grid is shown along this direction), and the y -axis shows the azimuth. The same color scale is adopted in all three panels. Time is in units of the binary’s orbital period before the hardening stage. The binary’s Hill radius is highlighted by a black circle, and a few streamlines in the frame rotating with the secondary are overplotted by white curves. The location of the circular streamline of the inner disc closest to the secondary is shown by a red curve.

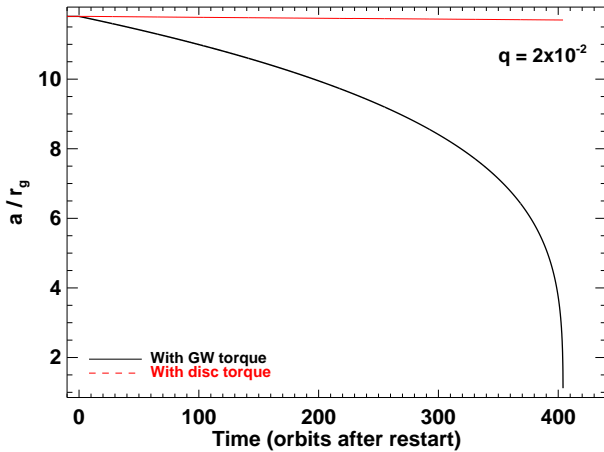


Figure 1. Time evolution of the binary’s semi-major axis, a , driven by the GW torque alone (black curve), and by the disc torque alone (red curve, both are results of simulations). Time is expressed in units of the binary’s orbital period at its initial separation, and a is shown in units of r_g .

radial direction, and it covers the full 2π range in azimuth with $N_\varphi = 780$ cells. A logarithmic spacing is used along the radial direction to optimize the grid’s resolution near the disc’s inner edge. The secondary’s Hill radius is resolved by about 30 grid cells along each direction at all times. Standard zero-gradient outflow boundary conditions are applied at the grid’s inner and outer edges.

4 RESULTS

Our simulations were performed in two steps. The secondary is first held on a fixed circular orbit about the binary’s center of mass. Its mass is gradually increased over 100 orbits to avoid a violent disc relaxation following the introduction of the sec-

ondary. The secondary progressively depletes a gap around its orbit, which attains a quasi steady-state density profile ~ 400 orbits after the insertion of the secondary. Simulations were then restarted with the binary feeling the gravitational wave torque only. This second stage, which we refer to as the hardening stage in what follows, lasts $\lesssim 410$ orbits, as indicated by Eq. (3). The disc torque on the secondary is discarded for simplicity, as $|\Gamma_{\text{disc}}| \ll |\Gamma_{\text{GW}}|$ from the binary’s initial separation. This point is clearly illustrated in Fig. 1, where we compare the time evolution of the binary’s semi-major axis when only the GW torque is included (black curve), and when only the disc torque is included (red curve).

Fig. 2 shows a time sequence of the gas surface density during the hardening stage. Time is expressed in orbital periods at the binary’s initial separation, a_0 . Streamlines in the frame rotating with the secondary are shown as white curves. The circulating streamline of the inner disc closest to the secondary is depicted by a red curve. This time sequence clearly shows no density increase in the inner disc, but underlines instead the progressive replenishment of the gap. The gas density inside the gap becomes more and more asymmetric as the binary’s hardening gets faster, with more gas behind the secondary ($\varphi < 0$) than ahead of it. This asymmetry results from fluid elements of the inner disc embarking onto horseshoe streamlines and being funneled to the outer disc or to the gap. This gap asymmetry is reminiscent of the one occurring during type III runaway migration (a fast, generally inward migration regime driven by the disc torque; see Masset & Papaloizou 2003).

Fig. 3 displays the azimuthally-averaged disc density at different times prior to the binary’s merger. It further illustrates that the rapid shrinkage of the binary does not squeeze the inner disc in our 2D simulations, in contrast to previous height-integrated 1D disc models (Armitage & Natarajan 2002; Lodato et al. 2009; Chang et al. 2010).

To gain further insight into the time evolution of the mass in the inner disc, we have performed simulations in which a small patch of the disc inside the inner separatrix of the horseshoe region is polluted initially with a passive contaminant

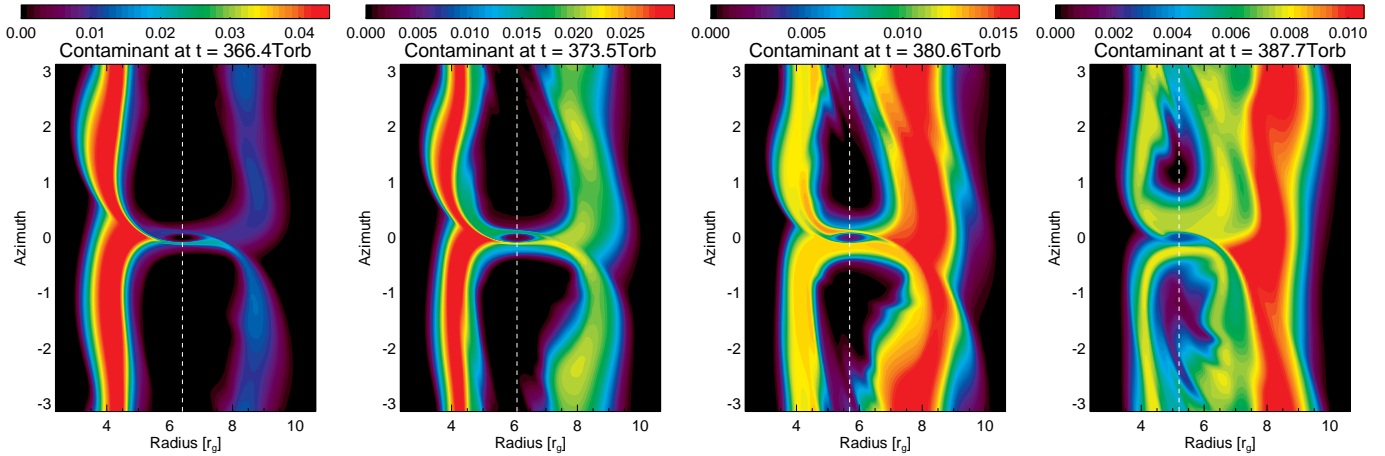


Figure 4. Time sequence showing the evolution of the specific concentration of the passive contaminant, C , defined in the text. The x -axis shows the radial coordinate in units of r_g , and the y -axis the azimuth. Contour levels are defined for each panel to underline the region occupied by the contaminant at each time. The binary's separation is indicated by a vertical dashed line.

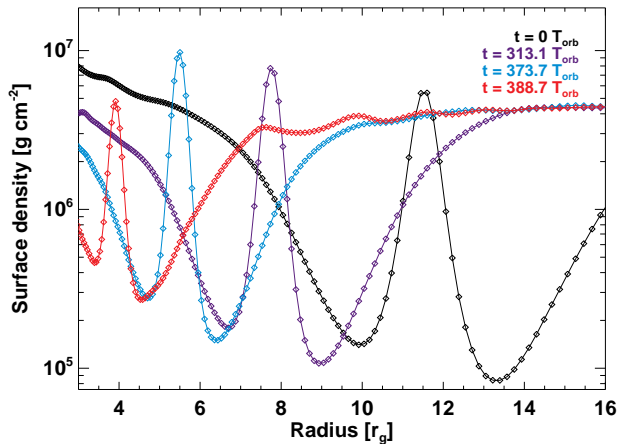


Figure 3. Azimuthally-averaged surface density at different times expressed in units of the binary's initial orbital period. Radius is in units of the Schwarzschild radius r_g . Density peaks correspond to gas accumulation inside the circum-secondary disc.

that is advected with the flow. We denote by ψ the concentration per unit area of the contaminant, and evolve the equation

$$\frac{\partial \psi}{\partial t} + \nabla \cdot (\psi \mathbf{v}) = 0. \quad (5)$$

Writing $\psi(r, \varphi) = C(r, \varphi) \Sigma$, where $C(r, \varphi)$ is referred to as the specific concentration of the contaminant, and using the continuity equation, Eq. (5) can be recast as $\partial_t C + \mathbf{v} \cdot \nabla C = 0$. The patch of contaminant is introduced 340 orbits after the beginning of the hardening stage, and the time evolution of its specific concentration, C , is displayed as a time sequence in Fig. 4. Time increases by ≈ 7 orbits moving from left to right through the panels. The location of the secondary is shown by a vertical dashed line in each panel. In the left-hand panel, most of the contaminant is concentrated inside the inner separatrix of the horseshoe region, located at $r \approx 4.5r_g$. At this time, a (relatively) tiny fraction of the contaminant is being funneled to the outer disc, and ends up sliding along the outer

separatrix of the horseshoe region at $r \approx 8r_g$. The second panel highlights that more and more contaminant is being redirected to the outer disc. As the binary continues hardening, most of the contaminant now moving in the outer disc remains in the outer disc, only a small fraction of it undergoes inward horseshoe U-turns back to the inner disc. In the third panel, most of the contaminant is now concentrated in the outer disc. The radial profile of the contaminant gets progressively thicker in the outer disc, because the outer separatrix of the horseshoe region is moving inwards faster than the contaminant may drift inward viscously. This is even more clear in the fourth panel of Fig. 4, where the contaminant in the outer disc is left well behind the secondary. We also mention that in addition to the material passing to the outer disc, we never observe the contaminant being pushed inward: the region below $r \sim 3.5r_g$ remains dark.

The time evolution of the gas surface density in Figs. 2 and 3, and of the contaminant's specific concentration in Fig. 4, suggest that most of the mass in the inner disc relative to the secondary is transferred to the outer disc through horseshoe streamlines. To help quantify this funneling mechanism, we display in Fig. 5 the time evolution of the mass in the inner disc, in units of the binary mass, during the last ~ 70 orbits before the binary's merger. The increase in the mass of the outer disc during the same time span (also in units of the binary mass) is overplotted by a red curve. The difference between both curves accounts for the mass lost from the computational grid, which is shown by a dashed curve in Fig. 5. These curves clearly show that the fraction of the inner disc's mass funneled to the outer disc largely exceeds that drained onto the primary.

5 CONCLUDING REMARKS

The minor merger of two galaxies leads to the formation of a supermassive black hole binary with unequal mass ratio embedded in a gaseous disc. The tidal interaction between the binary and the disc hardens the binary's orbit. When the binary gets sufficiently tight, emission of gravitational waves becomes the main source of angular momentum extraction from

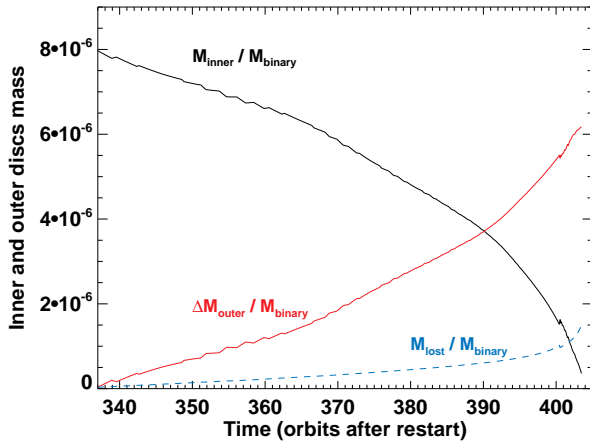


Figure 5. Mass of the inner disc during the ultimate stages of the binary’s hardening, before the secondary leaves the computational grid (black curve). The increase in the mass of the outer disc during the same time interval, namely $\Delta M_{\text{outer}} = M_{\text{outer}}(t) - M_{\text{outer}}(337T_{\text{orb}})$, with M_{outer} the outer disc’s mass, is displayed by a red curve. The mass lost from the computational grid during the same time interval is shown by a dashed curve. Masses are in units of the binary mass, and all curves have been smoothed over 5 orbits.

the binary’s orbit, and causes further rapid shrinkage until coalescence takes place.

We have focused in this Letter on the evolution of the disc region located between the primary and the secondary black holes (the inner disc), when the binary’s hardening is dominated by the emission of gravitational waves. With the help of 2D hydrodynamical simulations, we have shown that the rapid hardening of the binary does not lead to a significant squeezing of the inner disc. The latter is redirected instead toward the disc region beyond the secondary’s orbit (the outer disc) through horseshoe streamlines. When the binary’s hardening timescale driven by gravitational radiation becomes shorter than the disc’s viscous drift timescale, fluid elements in the inner disc embark on horseshoe trajectories with respect to the secondary, and are progressively funneled to the outer disc. The funneling of the inner disc toward the outer disc implies that, in contrast to the predictions of 1D disc models, the accretion rate onto the primary is not dramatically increased just prior to merger, and, as a result, the disc emission before the binary merger should remain at about the same level. After the merger, an electromagnetic afterglow could be detected as the disc gets accreted by the merged black hole (Milosavljević & Phinney 2005).

The physical model we have considered is a straightforward 2D extension of the model considered in Armitage & Natarajan (2002), Lodato et al. (2009), and Chang et al. (2010), and as was already pointed out by these authors, this model has a number of simplifying assumptions. We have considered an intermediate binary mass ratio ($q = 2 \times 10^{-2}$). A smaller mass ratio would decrease the binary’s separation below which a significant funneling occurs (which we have checked with additional simulations, not reported here). A mass ratio closer to unity would initially lead to a rapid depletion of the inner disc, and the binary would be surrounded by a circumbinary disc (e.g.,

MacFadyen & Milosavljević 2008; Cuadra et al. 2009), making our funneling mechanism not applicable. Also, different values of the disc aspect ratio and viscosity would change the structure of the gap opened by the secondary (width, depth). Partial gap-opening could occur in very thick discs, and a three-dimensional disc modeling would be valuable. In some cases, the disc-secondary interaction can make the outer disc eccentric, thereby driving the binary’s eccentricity (e.g., Papaloizou et al. 2001; Ogilvie & Lubow 2003), although the latter should be partially damped during the fast inspiral driven by gravitational radiation (Armitage & Natarajan 2005). Still it remains to be clarified how the funneling mechanism would operate in the presence of an eccentric binary.

ACKNOWLEDGMENTS

We thank P. Chang, J. Guilet, Z. Haiman, D. N. C. Lin, K. Menou, and E. Quataert for stimulating discussions, and the referee for useful comments. CB is supported by a Herchel Smith Postdoctoral Fellowship. ER-R acknowledges support from the David and Lucille Packard Foundation and the NSF grant: AST-0847563.

REFERENCES

- Armitage P. J., Natarajan P., 2002, *ApJL*, 567, L9
- Armitage P. J., Natarajan P., 2005, *ApJ*, 634, 921
- Begelman M. C., Blandford R. D., Rees M. J., 1980, *Nature*, 287, 307
- Chang P., Strubbe L. E., Menou K., Quataert E., 2010, *MNRAS*, 407, 2007
- Crida A., Morbidelli A., Masset F., 2006, *Icarus*, 181, 587
- Cuadra J., Armitage P. J., Alexander R. D., Begelman M. C., 2009, *MNRAS*, 393, 1423
- D’Angelo G., Bate M. R., Lubow S. H., 2005, *MNRAS*, 358, 316
- Gould A., Rix H.-W., 2000, *ApJL*, 532, L29
- Kazantzidis S., Mayer L., Colpi M., Madau P., Debattista V. P., Wadsley J., Stadel J., Quinn T., Moore B., 2005, *ApJL*, 623, L67
- Lacey C., Cole S., 1993, *MNRAS*, 262, 627
- Lin D. N. C., Papaloizou J., 1986, *ApJ*, 309, 846
- Lodato G., Nayakshin S., King A. R., Pringle J. E., 2009, *MNRAS*, 398, 1392
- MacFadyen A. I., Milosavljević M., 2008, *ApJ*, 672, 83
- Masset F., 2000, *A&AS*, 141, 165
- Masset F. S., D’Angelo G., Kley W., 2006, *ApJ*, 652, 730
- Masset F. S., Papaloizou J. C. B., 2003, *ApJ*, 588, 494
- Milosavljević M., Merritt D., 2001, *ApJ*, 563, 34
- Milosavljević M., Phinney E. S., 2005, *ApJL*, 622, L93
- Ogilvie G. I., Lubow S. H., 2003, *ApJ*, 587, 398
- Papaloizou J. C. B., Nelson R. P., Masset F., 2001, *A&A*, 366, 263